Caulollins from *Caulobacter crescentus*, a Pair of Partially Unstructured Proteins of $\beta\gamma$-Crystallin Superfamily, Gain Structure upon Binding Calcium†

Maroor K. Jobby and Yogendra Sharma*

Center for Cellular and Molecular Biology, Hyderabad 500007, India

Received May 4, 2007; Revised Manuscript Received August 8, 2007

ABSTRACT: The $\beta\gamma$-crystallin superfamily comprises members from various taxa and species, which have similar domain topologies as that of lens β- and γ-crystallins. We have studied new microbial members of this understudied $\beta\gamma$-crystallin superfamily from the bacterium *Caulobacter crescentus*. These proteins, which we named "caulollins", are paralogues with a single $\beta\gamma$-crystallin domain, made up of two Greek key motifs with AB-type arrangement seen in γ-crystallin. The second Greek key motif has Cys in place of a generally conserved Phe/Tyr residue, and the Tyr corner, considered important for the proper $\beta\gamma$-crystallin fold, is missing, making this a sequentially diverse atypical $\beta\gamma$-crystallin domain. This atypical domain binds two Ca^{2+} with moderate affinity (0.8−20 μM). In apo form, caulollins are partially unstructured proteins and gain structure upon binding Ca^{2+}. Unlike many other microbial $\beta\gamma$-crystallin domains, this domain is monomeric, though in the presence of Ca^{2+} it becomes more compact. Ca^{2+} binding increases the intrinsic stability of proteins, suggesting the role of Ca^{2+} as an extrinsic stabilizer. N-Terminal extension does not play any role in modulating Ca^{2+} binding, intrinsic stability, or oligomerization. We noted that there are several such variant domains in the genomes of unrelated species. It appears that caulollins along with these members form a subfamily in the $\beta\gamma$-crystallin superfamily that would be partially unstructured in apo form, unlike many other domains from lens or microbial crystallins. This work further suggests that Ca^{2+} binding is a widespread feature of the $\beta\gamma$-crystallin superfamily.

The $\beta\gamma$-crystallin superfamily represents diverse proteins containing crystallin-type Greek key motifs. These proteins are all β-sheet proteins containing two, four-stranded Greek key motifs forming one $\beta\gamma$-crystallin domain. β- and γ-crystallins from eye lens are the representative and founding members of this superfamily (*1*, *2*). Although crystallins from eye lens have been extensively studied, only few members from non-lens tissues have been described and studied. These non-lens proteins have been reported from diverse organisms and tissues (*3*). Some of the eukaryotic and microbial $\beta\gamma$-crystallin domains have been shown to bind Ca^{2+} (*4*−*7*). However, Ca^{2+} binding is still not considered an innate property of this superfamily (*3*, *8*, *9*). Therefore, it is essential to characterize more diverse proteins of the superfamily to evaluate Ca^{2+}-binding properties of these $\beta\gamma$-crystallin domains apart from understanding their sequence−structure relationship.

On the basis of the sequence alignment of lens β- and γ-crystallins, the conserved residues and signature sequence deemed essential for the formation of the $\beta\gamma$-crystallin fold have been identified (*10*). However, in recent years, a few $\beta\gamma$-crystallin domains have been described that lack some of these conserved residues of this fold. These include the first $\beta\gamma$ domain, AIM1-g1 from the protein AIM1, lacking the conserved aromatic and Gly residues in the sixth and eighth position in its first Greek key motif followed by a insertion of about 10 residues in the region between Gly-8 and Ser-34 (*11*). In spite of these variations, this domain folded as an all β-sheet protein and was shown to bind Ca^{2+} (*5*). Similarly, D1 and D2 domains of *Yersinia* crystallin do not have the conserved Tyr corner present in a typical $\beta\gamma$-crystallin domain, yet these proteins gain β-sheet conformation in Ca^{2+}-bound form (*6*). Therefore, the role of signature residues for the folding of a $\beta\gamma$-crystallin domain and Ca^{2+} binding need to be examined by studying more examples of naturally occurring variant $\beta\gamma$-crystallin domains.

The limits of relationship between sequence and structure and its effect on Ca^{2+} binding and stability are important aspects that need to be addressed in this superfamily. Proteins having substitutions at key positions in a $\beta\gamma$-crystallin domain provide natural examples of mutations and selection, which offer an opportunity to study the importance of conserved residues at those positions. Confirmation of Ca^{2+} binding to these variant proteins would also shed more light on this superfamily as a family of Ca^{2+}-binding proteins, as well as on the evolution and fine-tuning of the functional property in these otherwise structural proteins. It is in this connection that we analyzed the genome sequences for the presence of putative members of the $\beta\gamma$-crystallin superfamily with variations and identified a pair of proteins from the bacterium *Caulobacter crescentus*.

† This research is supported by a grant from the Department of Science and Technology (DST), Government of India. M.K.J. is a recipient of a senior research fellowship from the CSIR, Government of India.

* Address correspondence to this author: Center for Cellular and Molecular Biology, Uppal Road, Hyderabad-500007, India; phone +91-40-2716 0222; fax +91-40-2716 0591; e-mail yogendra@ccmb.res.in.

10.1021/bi700843q CCC: $37.00
Published on Web 10/04/2007

Caulobacter crescentus, a single-celled bacterium, is a model organism for studying asymmetrical cell division and cell cycle (*12*, *13*). It can survive under low nutrient environmental conditions in aquatic habitats. It secretes proteins forming an outer cell envelope known as the S-layer, a two-dimensional paracrystalline array of proteins that requires Ca^{2+} for crystallization (*14*). Although this phenomenon has been known from a long time and some of the components of S-layer have been identified, many questions remain unanswered about the contribution of other proteins involved in calcium physiology and metabolism. Ca^{2+} is also essential for stalk development in *Caulobacter* species (*15*). It is with these objectives that the genome of *C. crescentus* was sequenced to decipher its proteome (*16*). We have studied a pair of $\beta\gamma$-crystallin proteins from this species and compared it to their homologues from eukaryotes and microbes. In these proteins, which we have named "caulollins", the typical conserved aromatic residue at the start of the second Greek key motif is substituted by Cys and the characteristic tyrosine corner is absent, making them interesting for understanding their Ca^{2+}-binding properties with respect to other members.

In this paper, we report the conformation, stability, and Ca^{2+} binding of two paralogues of $\beta\gamma$-crystallins (caulollins) that differ in the length of N-terminal extension, identified in the proteome of proteobacterium *C. crescentus* (*16*). We demonstrate that these proteins bind Ca^{2+} with micromolar affinity. These $\beta\gamma$-crystallin domains are partially unstructured and gain structure upon binding Ca^{2+}. Ca^{2+} binding stabilizes the protein and increases compactness. Our results on caulollins along with earlier data on Ca^{2+} binding to several proteins of this superfamily strongly suggest that Ca^{2+} binding is a prevalent property of the $\beta\gamma$-crystallin superfamily. Furthermore, our studies point to the presence of a subfamily of unstructured domains in the absence of Ca^{2+} within the $\beta\gamma$-crystallin superfamily.

MATERIALS AND METHODS

Identification and Selection of $\beta\gamma$-Crystallin Domains from Caulobacter crescentus. We performed a BLAST (*17*) search against the genome sequence of the bacterium *C. crescentus* strain CB15 (*16*) with a γ-crystallin sequence. Crystallin-type Greek key motifs occur in pairs, and each motif is about 35−40 residues in length with a signature sequence of XXXXX**Y/F**XXXX**F/Y**X**G** at the beginning and a conserved Ser at about the 34th position in a stretch of D/NXXSS. We found two proteins with paired Greek key motifs. These proteins were named as caulollin-1 (accession number NP_419839, locus tag CC1023) and caulollin-2 (accession number NP_419840, locus tag CC1024). The putative $\beta\gamma$-crystallin domain (residue 103−180) of caulollin-2 is named as caulollin-2D. The protein sequence of caulollins was used as a template to identify similar proteins of the $\beta\gamma$-crystallin superfamily from the database.

Cloning, Expression, and Purification of Caulollins. Genomic DNA of *C. crescentus* was a kind gift from Professor Lucy Shapiro, Stanford University. Primers were designed to amplify full-length as well as $\beta\gamma$ domain regions of both proteins from the genomic DNA via PCR;[1] the resulting DNA was ligated into expression vector pET21a (Novagen) under T7 promoter. The expression constructs were transformed to *Escherichia coli* strain BL21(DE3) RIL codonplus (Stratagene Inc). The transformed *E. coli* cells were grown to mid-log phase in Terrific broth, and heterologous protein expression was induced by IPTG. The cultures were harvested after 3 h, and the cell pellet was stored at −80 °C. We could not see any overexpression of full-length caulollin-2 on an SDS−polyacrylamide electrophoretic gel; however, its $\beta\gamma$-crystallin domain (caulollin-2D) was overexpressed. Conversely, only full-length caulollin-1 was overexpressed while its $\beta\gamma$-crystallin domain was not.

Both proteins were found to be localized in inclusion bodies in *E. coli*. After cell lysis in 20 mM Tris-HCl (pH 7.5), 100 mM NaCl, and 1 mM EDTA by sonication, the pellets were washed with lysis buffer containing 1% Triton X-100 and then subsequently with Triton X-100-free buffer. The washed inclusion bodies were stored at −30 °C till further used.

A modification of the on-column refolding method (*18*) was employed for refolding and purification of proteins. For purification, a washed pellet of caulolin-1-containing inclusion bodies was suspended in 10 mM Tris-HCl (pH 7.5) buffer containing 1 mM EDTA, 8 M urea, and 1 mM TCEP for 5−6 h at room temperature (RT). The solublized inclusion body was centrifuged and the supernatant pH was adjusted to 12 by addition of NaOH before the sample was loaded on a Q-Sepharose FF column equilibrated in the same buffer. Under these conditions, most of the protein bound to the column. After being washed with the start buffer to remove unbound proteins, the column was washed with start buffer without urea and TCEP. The bound protein was then eluted with a linear gradient of 0−500 mM NaCl. The protein was further purified on a Superdex-75 (GE Life Sciences) column equilibrated in 20 mM Tris-HCl (pH 7.5) containing 100 mM KCl. The purified protein was concentrated, decalcified, and used immediately for Ca^{2+}-binding studies. All the buffers used in the studies were passed through a Chelex-100 column (Bio-Rad) to remove traces of Ca^{2+}.

A similar method of oxidative on-column refolding was employed for the refolding of caulollins-2D. All the steps were same as those used for caulollin-1 purification except DTT was used instead of TCEP during the solubilization of inclusion bodies and pH adjustment of solublized inclusion bodies was not required. A linear gradient of 0−1 M NaCl was used to elute the protein. After decalcification, the protein was used immediately for binding and spectral studies. The yield of both proteins was about 1 mg/L of culture.

^{45}Ca Overlay Assay. An earlier protocol of Maruyuma et al. (*19*) was used with minor modifications. Protein (50 μg) was spotted on a PVDF membrane and washed with buffer containing 10 mM imidazole hydrochloride (pH 7.1) and 2 mM $MgCl_2$. The blot was incubated with the above buffer containing 1 μCi of ^{45}Ca (New England Nuclear) for 10 min

[1] Abbreviations: PCR, polymerase chain reaction; IPTG, isopropyl thio- β-D-galactoside; EDTA, ethylenediaminetetraacetic acid, TCEP, tris(2-carboxyethyl)phosphine hydrochloride; DTT, dithiothreitol; PVDF, poly(vinylidene difluoride); CD, circular dichroism; ITC, isothermal titration calorimetry; DSC, differential scanning calorimetry.

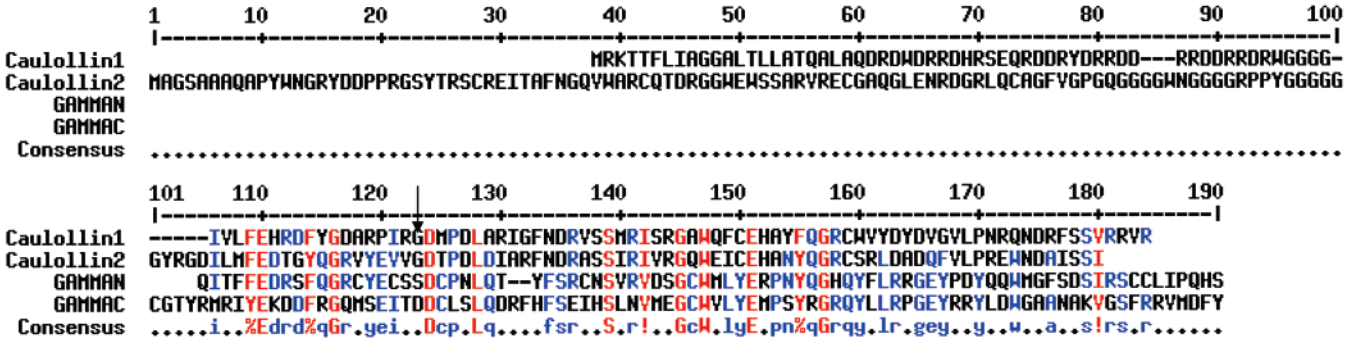

FIGURE 1: Sequence alignment of caulollin-1 and -2 with the N- and C-terminal domain of γ-crystallin. Arrow indicates the position of mutation (G123D) in caulollin-2D starting from residue 103 of caulollin-2.

at room temperature. The blot was then washed twice with 50% ethanol, air-dried, and scanned in a phosphorimager (Fuji FLA-3000).

Fluorescence Spectroscopy. Fluorescence emission spectra were recorded on a Hitachi F-4500 spectrofluorometer. The cuvettes were soaked in 10 mM EDTA solution and rinsed with Chelex-100-treated MQ water (Millipore Inc.). The spectra were recorded in the correct spectral mode of the instrument with excitation and emission band passes of 5 nm. All measurements were done at room temperature.

Terbium Binding. Tb^{3+} binding to both proteins was monitored on a Hitachi F-4500 spectrofluorometer. The excitation wavelength was 285 nm with bandpasses of 5 nm for both excitation and emission. The titration buffer consisted of 10 mM Tris-HCl (pH 7.4) and 10 mM KCl. Aliquots of $TbCl_3$ from a stock solution were added and the solution was incubated for 5 min before the spectra were recorded.

Circular Dichroism Spectroscopy. Far- and near-UV CD spectra of both proteins were recorded at room temperature on a Jasco-715 spectropolarimeter with 0.1 and 1 cm path length cuvettes, respectively. Appropriate buffer spectra were recorded and subtracted from the protein spectra. Secondary structure fractions from corrected far-UV CD spectra were calculated by use of CDNN software based on neural networks (*20*).

Analytical Gel Filtration. Hydrodynamic volumes of protein were determined on a Superdex G-75 (GE Life sciences) column, calibrated with standard molecular weight markers. The elution buffer used was 50 mM Tris-HCl (pH 7.5), 100 mM KCl, and 1 mM EDTA. EDTA was replaced with 10 mM $CaCl_2$ for holoproteins.

Isothermal Titration Calorimetry. Dissociation constants were determined from the binding isotherm of Ca^{2+} and proteins in a VP-ITC calorimeter (Microcal Inc.). Ligand and protein solutions were prepared in 10 mM Tris-HCl (pH 7.5) containing 50 mM KCl. All titrations were carried at 25 °C. Caulollin-1 (43 μM) in the sample cell was titrated with 41 injections, 3 μL each, of 3 mM $CaCl_2$. Caulollin-2D (68 μM) was titrated with 90 injections, which included 70 injections of 2 μL, followed by six injections of 3 μL and the rest of 4 μL, from 2 mM $CaCl_2$ solution loaded in the syringe. Appropriate buffer titrations were carried out to determine the heat of dilution and subtracted from the Ca^{2+}-binding thermograms before analysis of the data by Microcal Origin 7.0.

Differential Scanning Calorimetry. DSC was carried on a VP-DSC calorimeter (Microcal Inc.). Buffer baseline was established from Chelex-100-treated 10 mM Tris-HCl (pH 7.6) containing 50 mM KCl for experiments with apoproteins. $CaCl_2$ (8 mM) was added to the buffer for scanning with holoproteins. The scan rate was 60 °C/h. The concentration of caulollin-1 used was 18 μM. Protein concentrations were 19.4 and 17 μM for apo- and holocaulollin-2D, respectively.

RESULTS AND DISCUSSION

With the completion of genome sequences of several species, the next task has been to explore the functions of newly identified genes. We have been interested in identifying the functions of the genes belonging to the $\beta\gamma$-crystallin superfamily. In this work, we have identified two members of $\beta\gamma$-crystallins in the genome sequence of *Caulobacter crescentus* (*16*) and characterized them as Ca^{2+}-binding proteins of this superfamily.

Caulollins as Novel members of $\beta\gamma$-Crystallins. Genome sequence of *C. crescentus* CB15 revealed the presence of two proteins containing putative $\beta\gamma$-crystallin domain annotated as $\beta\gamma$-crystallin proteins with locus tags CC1023 and CC1024 (*16*). Both proteins are paralogues and are contiguous in the genome. We have named these proteins as caulollin-1 and -2, (*Caulobacter* + crystallin). Sequence alignment of full-length caulollins with N- and C-terminal domains of bovine γ-crystallin is shown in Figure 1. Both proteins have long N-terminal extensions of 60 and 100 amino acids, respectively, followed by a single crystallin domain at the C-terminus; these have high identity and similarity to each other.

According to the sequence alignment of archetype lens β- and γ-crystallins, some residues identified as conserved in the $\beta\gamma$-crystallin motifs are F or Y at positions 6 and 11 (though F or Y is not always present at position 11), Gly13, and Ser34 (*10*). One unique feature of the $\beta\gamma$-crystallin domains of caulollins is the substitution of F/Y at position 6 with a Cys residue in the second Greek key motif (Figure 1). It is believed that this conserved aromatic residue with a bulky hydrophobic side chain is important for the folding of the $\beta\gamma$-crystallin domain (*10*, *21*). The arrangement of Greek key motifs in these caulollins is AB-type with a characteristic presence of a Trp corner in the second (B-type) Greek key motif (*22*). However, both proteins lack the characteristic tyrosine corner usually present in the B-type Greek key motifs (with a sequence of GXY) in β- and γ-crystallins, which is considered important for the folding and stability of such proteins (*23*, *24*). Caulollins are also

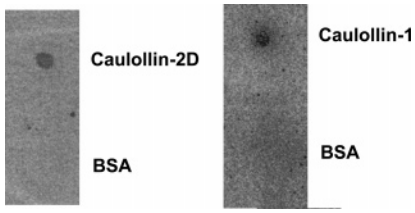

FIGURE 2: ^{45}Ca overlay assay: 50 μg of each protein was spotted on PVDF membrane before incubation in 10 mM imidazole hydrochloride (pH 7.1) and 2 mM $MgCl_2$ containing $^{45}CaCl_2$. Bovine serum albumin was used as a negative control. The signal was read in a phosphorimager.

rich in Arg residues (12−20%), mostly concentrated in the N-terminal arm. These features make these proteins interesting to compare with other members of $\beta\gamma$-crystallin superfamily.

We have studied these proteins for the effect of substitutions, deletion, and N-terminal extension on the conformation, Ca^{2+} binding, and domain−domain interaction.

Protein Preparation. We attempted recombinant protein production of full-length as well as crystallin domains in *E. coli*. However, we were unable to produce full-length protein of caulollin-2 or $\beta\gamma$-crystallin domain of caulollin-1. Full-length caulollin-1, referred to as caulollin-1, and $\beta\gamma$ domain of caulollin-2, referred as caulollin-2D (residue 103−180 of caulollin-2; residue 103 is the starting Met in recombinant caulollin-2D), were produced as inclusion bodies in *E coli.* Thus, caulollin-1 contains an N-terminal extension of 40 amino acids to the crystallin domain homologous of caulollin-2D. We have used modification of on-column refolding technique described earlier (*18*) for oxidative refolding and purification of proteins.

Similarly when overexpressed in *E coli*, the wild-type caulollin-2D was found to be truncated and appeared as a 6 kDa protein upon SDS−PAGE. However, we found a mutation, caulollin-2D G21D (G123D in caulollin-2 sequence), which expressed as a 9.5 kDa protein as expected from its sequence. This mutant protein was used in this study and is referred to as caulollin-2D. Caulollins degraded in 2−3 days, probably due to the presence of scissile peptide bonds of Arg, Asp, and Gly.

Caulollins Are Ca^{2+}-Binding Proteins. Since lens β- and γ-crystallins are known to bind Ca^{2+} ions (*4*, *25*−*27*), we have therefore, investigated whether these variant domains bind Ca^{2+}. We have used various specific binding assays to determine Ca^{2+} binding to these proteins. These included calcium-45 overlay assay, Tb^{3+} binding, and ITC. As shown in Figure 2, radioactive calcium ($^{45}Ca^{2+}$) binds to the immobilized protein on PVDF membrane.

We have also used Ca^{2+}-mimic Tb^{3+} to ascertain the cation binding to caulollins. Tb^{3+} and Ca^{2+} have similar ionic radii, but Tb^{3+} exhibits a phenomenon of lanthanide resonance energy transfer (LRET), a type of FRET, which is used to monitor its occupation of Ca^{2+}-binding sites in proteins. Tb^{3+} has been widely employed for investigating the Ca^{2+}-binding properties of several proteins (*28*). Tb^{3+} binding to caulollins results in increased luminescence intensity at 491 and 547 nm with decreased Trp emission intensity (Figure 3). This is a well-established method of determining Ca^{2+} binding to proteins (*29*). Tb^{3+} binding to these proteins results in a blue shift of Trp wavelength maxima, indicating the burial of Trp residues in the nonpolar core upon lanthanide binding (Figure 3).

Caulollins Bind Two Ca^{2+}. We determined the binding affinity of Ca^{2+} to caulollin-2D using ITC (Figure 4). The data fit best to the two-site sequential binding model. The dissociation constants of Ca^{2+} for caulollin-2D were 26.8 and 2 μM (Table 1). The affinity is comparable to several other members of this superfamily, such as β-crystallins (*25*), γ-crystallin (*4*), *Yersinia* crystallin (*6*), and protein S (*30*). It confirms that the absence of conserved aromatic residues, which have been believed to be important for the folding of crystallin domain, has not affected the Ca^{2+}-binding site.

We further studied the role of N-arm on modulating Ca^{2+}-binding affinity. Till now, there has not been any such study to understand the role of such extensions on Ca^{2+} binding, since most of these studies were performed either on single-domain or two-domain proteins. As seen in Figure 4b and Table 1, the number of binding sites is not altered due to N-terminal extension, indicating that crystallin domain forms the binding site. The Ca^{2+}-binding affinity of the first site is higher than that of caulollin-2D, whereas it remains the same for the second site (Table 1). Ca^{2+} binding to caulollins was enthalpically and entropically favored.

Caulollins Are Partially Unstructured in Apo Form and Gain Structure upon Binding Ca^{2+}. We have used CD spectroscopy and Trp emission fluorescence spectroscopy to investigate the effects of amino acid substitution (Cys in place of Y or F in the second Greek key motif) on Ca^{2+} binding and conformation of these proteins. Far-UV CD spectrum of apocaulollin-2D has a minimum at 203 nm (Figure 5), suggesting that caulollins are partially unstructured in the absence of Ca^{2+}. Ca^{2+} binding results in decreased intensity at 203 nm and appearance of two minima at 208 and 218 nm, characteristic of the β-sheet structure. Secondary structure fractions of apo- and holoproteins, calculated with the CDNN program (*20*), indicated that turns (26.2%) and unstructured fractions (37.8%) are higher in the apo form and decrease upon Ca^{2+} binding, increasing the antiparallel β-sheet content (29.9%) largely at the expense of these fractions and helices to a minor extent (Table 2). N-Terminal extension at the crystallin domain in caulollin-1 had no significant effect on the secondary structure of the apo- and holoprotein compared to the isolated domain (i.e., caulollin-2D). Similar effects of increased β-sheet content at the expense of turns and unstructured fractions were seen in caulollin-1 upon binding Ca^{2+} (Table 2). It appears that apo-$\beta\gamma$-crystallin domains in these proteins, which are highly similar in sequence, are partially unstructured, whereas they gain β-sheet conformation upon Ca^{2+} binding. These results further suggest that the presence of the N-terminal arm does not significantly affect the conformation and Ca^{2+} binding to crystallin domains in caulollins.

The near-UV CD spectrum of apocaulollin-2D with two minima at 298 and 280 nm and a maximum at 288 nm indicates a packed environment around aromatic side chains of Tyr and Trp residues (Figure 6). A broad peak around the 255−270 nm region indicates contribution of Phe and Cys residues. Ca^{2+} binding results in significant changes in the aromatic side-chain interactions in caulollin-2D. The CD spectrum of Ca^{2+}-bound protein showed similar minima and maxima as that of apoprotein but with lower intensity. Apocaulollin-1 has two minima at 292 and 282 nm and a

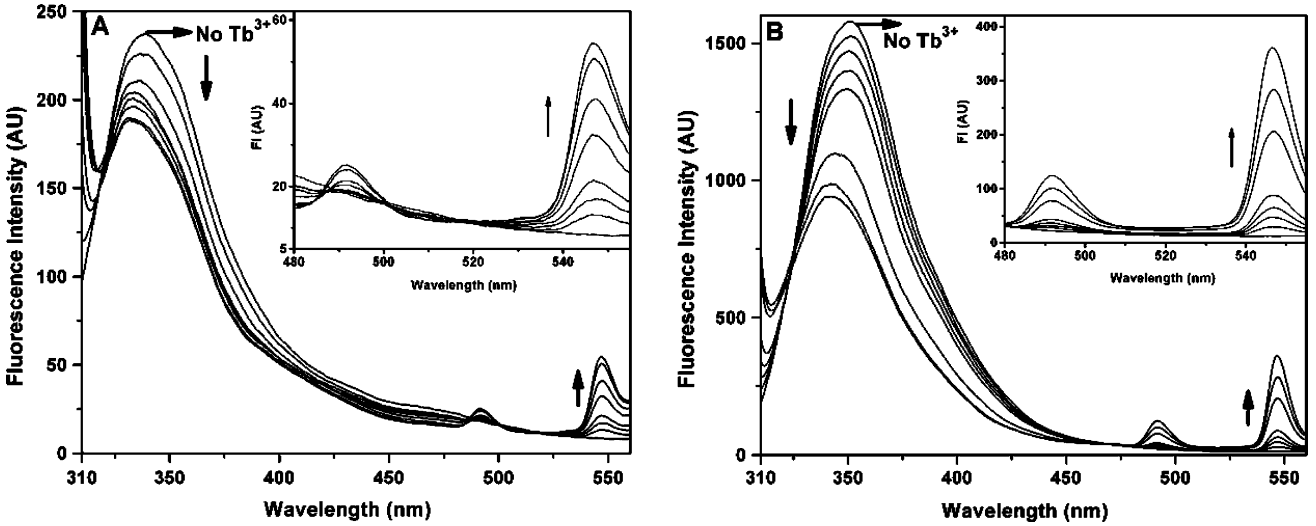

FIGURE 3: Terbium binding assay to (A) caulollin-2D and (B) caulollin-1. Aliquots of $TbCl_3$ were added from a stock solution and spectra were recorded till saturation was reached. The excitation wavelength was 285 nm, and spectra were recorded from 300 to 560 nm. Inset in each figure shows the region from 480 to 560 nm. Note the blue shift in Trp emission followed by a decrease in intensity (due to energy transfer) with concomitant increase at 491 and 547 nm. Arrows indicate the increasing concentrations of terbium.

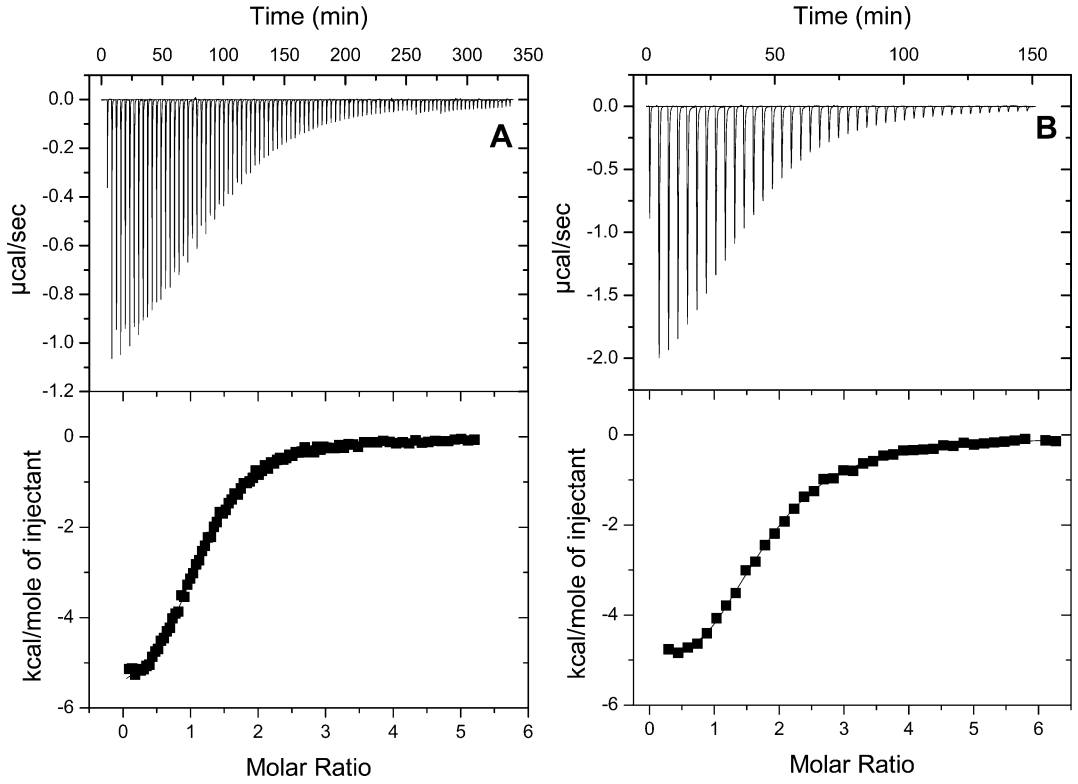

FIGURE 4: Isothermal titration calorigram of Ca^{2+} binding to (A) caulollin-2D and (B) caulollin-1: Protein and ligand were prepared in 10 mM Tris-HCl (pH 7.5) containing 50 mM KCl. Caulollin-1 (43 μM) in the sample cell was titrated with 41 injections, 3 μL each, of 3 mM $CaCl_2$. Caulollin-2D (68 μM) was titrated with 90 injections, which included 70 injections of 2 μL followed by six injections of 3 μL and the rest of 4 μL each, with 2 mM $CaCl_2$ stock solution in the syringe. The data were analyzed by use of the software Origin 7. Both data best fit to the two-site sequential binding model. The best-fit parameters are listed in Table 1.

maximum at 288 nm, similar to apocaulollin-2D (Figure 6). Ca^{2+} binding results in perturbation of aromatic side-chain interactions in both proteins.

The difference in the near-UV CD spectra of both caulollins could be due to the presence of two additional Trp and one Tyr in the N-terminal arm of caulollin-1, which also contribute to the signal in this region. Since Ca^{2+} perturbs the near-UV CD spectra in both cases, we suggest that the terminal extension does not play a role in modulating structural transitions, which are likely to be localized in the

Table 1: Thermodynamic Parameters of Ca^{2+} Binding to Caulollins Calculated from ITC

	caulollin-1	caulollin-2D
$K1$ (M)	$(8.62 \pm 1.63) \times 10^{-7}$	$(2.0 \pm 0.1) \times 10^{-6}$
$\Delta H1$ (kcal/mol)	-4.97 ± 0.05	-5.53 ± 0.03
$\Delta S1$ (cal mol^{-1} K^{-1})	11.1	7.52
$K2$ (M)	$(2.13 \pm 0.06) \times 10^{-5}$	$(2.68 \pm 0.22) \times 10^{-5}$
$\Delta H2$ (kcal/mol)	-5.36 ± 0.07	-1.53 ± 0.04
$\Delta S2$ (cal mol^{-1} K^{-1})	3.39	15.8

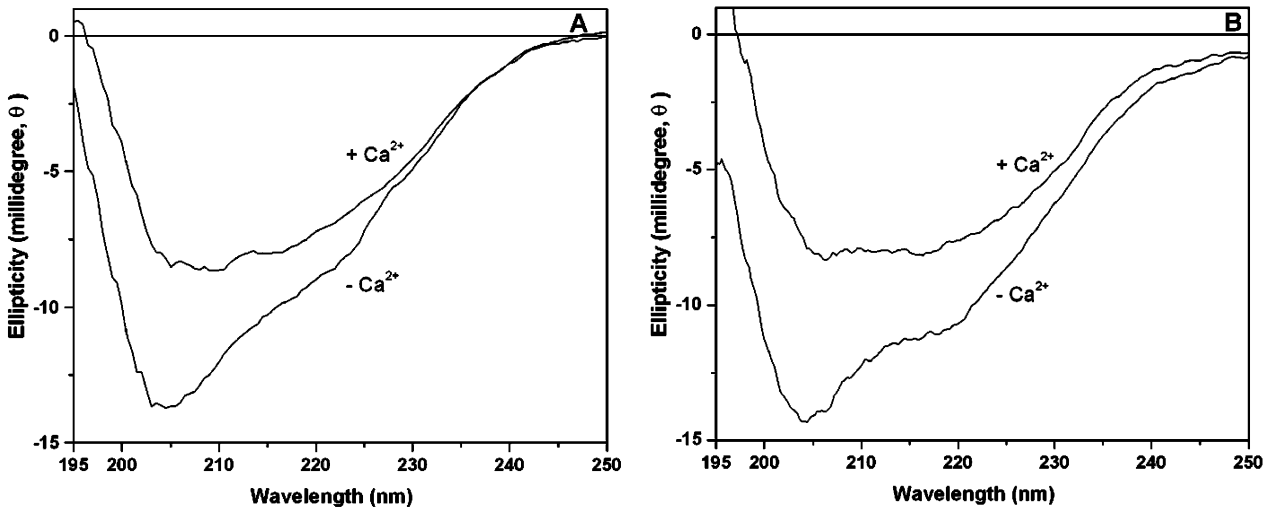

FIGURE 5: Far-UV CD spectra of caulollins: 0.15 mg/mL each (A) caulollin-2D and (B) caulollin-1 in 10 mM Tris-HCl (pH 7.5) containing 50 mM KCl were used to record spectra in a 0.1 cm path length cuvette. For studying the effect of Ca^{2+}, $CaCl_2$ was added to a final concentration of 2 mM in protein solution. Ellipticity is represented in millidegrees.

Table 2: Secondary Structure Composition of Apo- and Holocaulollins[a]

	% helix	% antiparallel	% parallel	% β-turns	% random coil
caulollin-1 apo	13.7	17.1	4.3	25	39.1
caulollin-1 holo	13.5	24.50	5.2	21	35.1
caulollin-2D apo	12.0	21.9	3.6	26.2	37.8
caulollin-2D holo	10.6	29.9	3.8	21.9	34.6

[a] These parameters were calculated from far-UV CD spectra by use of the program CDNN (*20*).

$\beta\gamma$-crystallin domain. It is known that Ca^{2+} binds at the Greek key motif as suggested earlier in case of some homologous protein members (*4*).

Trp fluorescence (emission maxima and intensity) is sensitive to its microenvironment. Apocaulollins display Trp emission maxima at 342 nm, indicating partial solvent exposure of this aromatic residue (Figure 7). Addition of Ca^{2+} shifts the emission maximum to 338 nm with a decrease in the intensity. These changes indicate that Ca^{2+} binding causes structural rearrangements in the vicinity of Trp residues, such as burial of Trp in the hydrophobic interior of protein. The presence of charged residues flanking the Trp may explain the quenching of intensity upon Ca^{2+} binding in both proteins. Tb^{3+} binding also resulted in a similar blue shift of the Trp emission maxima (Figure 3), indicating that these ions play structural roles in stabilizing the domain.

Results from CD and fluorescence spectroscopy indicate that, in the apo form, caulollins are partially unstructured proteins that are stabilized by Ca^{2+} binding.

N-Terminal Extension of $\beta\gamma$-Crystallin Domains Plays No Role in Determining the Quaternary Structure. Caulollin-1 and -2D share a high degree of sequence homology in the core crystallin domain. However, the difference is the presence of an N-terminal extension (40 residues) in caulollin-1. It has been shown earlier that terminal extension plays an important role in the oligomerization of lens β-crystallins (*31*, *32*). We have, therefore, investigated the role of the N-terminal arm on the oligomerization of caulollins using analytical gel-filtration chromatography. Apocaulollin-2D (molecular mass 9.5 kDa) has a lower elution volume than the holo form (Figure 8A). However, molecular mass standards used for calibrating the elution volume indicated that both apo and holo forms are monomeric under these conditions. Elution volume for the apo form is greater than for the holoprotein, probably due to its partially unstructured nature. It appears that the holoprotein is more compact than the apo form. Both apo and holo forms of caulollin-1 (molecular mass 16.5 kDa) have elution volumes higher than that of RNase A (13.7 kDa) but less than that of chymotrypsinogen (25 kDa) (Figure 8B), though in the case of the holoprotein, some fraction of dimer species could be present (Figure 8). Thus, both forms of caulollins are largely monomeric, though with different hydrodynamic volumes. It is known that unstructured proteins elute at lower elution volume than expected for monomers of their molecular mass (*33*). Fluorescence and CD spectroscopy had indicated significantly increased β-sheet content in caulollins upon Ca^{2+} binding. Analytical gel filtration confirms such structural changes leading to compaction of the proteins and hence the higher elution volume. These data further suggest that variant crystallin domain of caulollins, with or without N-terminal extension, do not interact intramolecularly as seen in the case of some eukaryotic $\beta\gamma$-crystallin domains, such as β-crystallins (*34*), AIM1-g1, and AIM1-g5 (*5*, *35*).

Ca^{2+} Acts as an Extrinsic Stabilizer. We have carried out thermal unfolding studies of caulollins by DSC. All thermal denaturations were found to be reversible and fit best to a two-state unfolding model. Ca^{2+} binding increases the T_m of caulollin-2D by 15−72 °C, accompanied by a 3-fold increase in the calorimetric enthalpy (Table 3). The ratio of van't Hoff enthalpy to calorimetric enthalpy ($\Delta H_v/\Delta H_{cal}$) for apo- and holocaulollin-2D was greater than 1 (2.4 and 2.7, respectively), indicating the presence of aggregates (*36*, *37*). Since analytical gel filtration did not show the presence of any oligomers, it is possible that weakly associated intramolecular aggregates were present during the scan, which do not interfere with the reversibility of the protein denaturation.

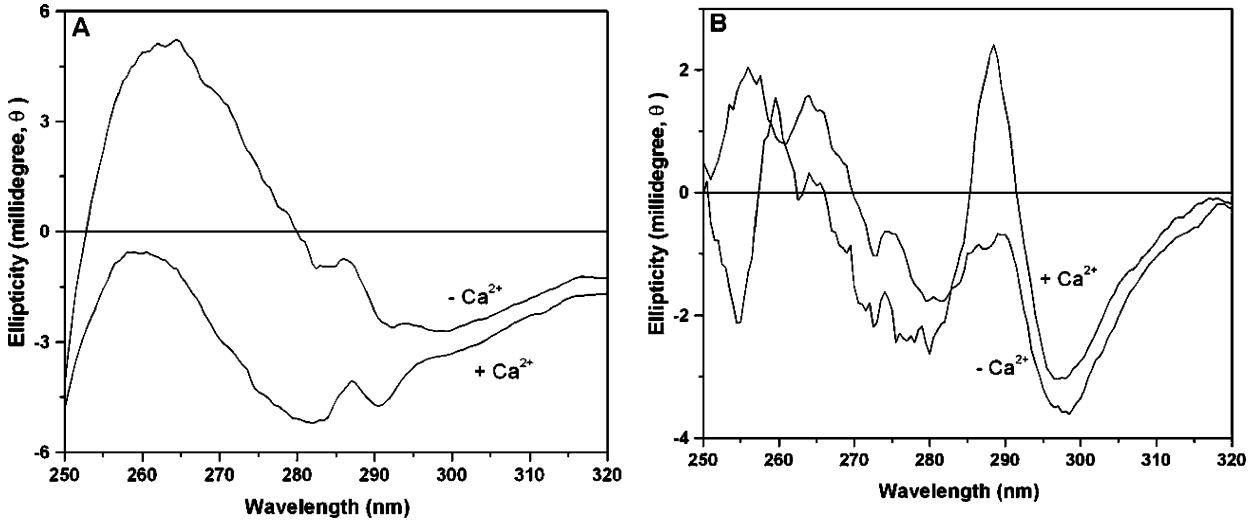

FIGURE 6: Near-UV CD spectra of caulollins: (A) 0.6 mg/mL caulollin-2D and (B) 0.5 mg/mL caulollin-1 prepared in the same buffer as for far-UV CD spectra. $CaCl_2$ was added to the apoprotein to a final concentration of 2 mM.

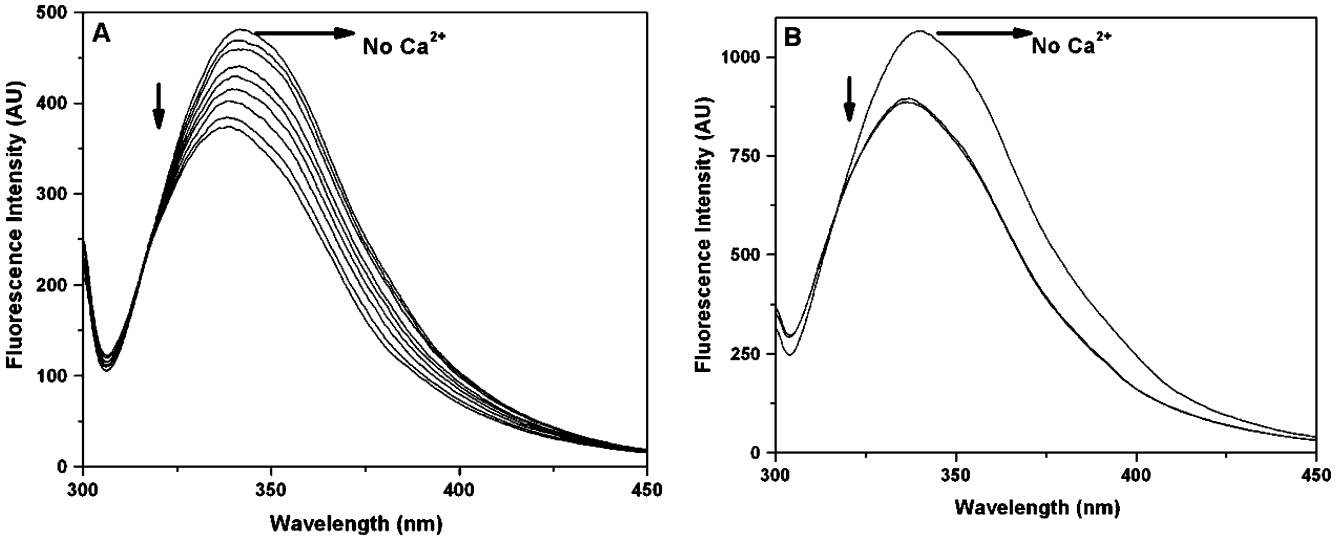

FIGURE 7: Trp fluorescence emission spectra of apo- and holo- (A) caulollin-2D and (B) caulollin-1: Increasing concentrations of $CaCl_2$ were added to the solution (indicated by arrow) containing 40 μg of protein, and spectra were recorded by excitation at 295 nm in the correct spectral mode. Note the decrease in intensity with blue shift of wavelength maxima.

Presence of the N-terminal arm in caulollin-1 did not significantly affect the T_m of either apo- or holoproteins compared to caulollin-2D (Table 3). Apocaulollin-1 showed higher ΔH_{cal} compared to apocaulollin-2D, and the $\Delta H_v/\Delta H_{cal}$ ratio was 1, indicating a monomeric unfolding unit, whereas parameters obtained for holoprotein denaturation were similar to that of holocaulollin-2D. These results indicate that the N-terminal arm does not play a role in stabilizing the $\beta\gamma$-crystallin domain. Detailed studies on the scan rate and concentration dependence on the thermal denaturation could not be carried out due to low yield of proteins.

Putative Ca^{2+}-Binding Sites. Due to the poor yield and degradation of proteins, we could not proceed with structure determination by crystallography or NMR. In the absence of a 3D structure, we attempted to build a hypothetical model for caulollin-2D. Like protein S and spherulin 3a, the sequence signature NDXXSS, known to be involved in Ca^{2+} ligation, is present in both Greek key motifs of caulollins. On this basis, we suggest that the putative Ca^{2+}-binding residues in caulollins should be homologous to those in protein S (*38*), spherulin 3a (*8*), or ciona crystallin (*9*), which are indicated by asterisks in Figure 9.

Caulollins as Representative Members of a Subfamily of Partially Unstructured Proteins of $\beta\gamma$-Crystallins. We have described the conformation and Ca^{2+}-binding properties of a variant protein of $\beta\gamma$-crystallin superfamily that lacks a conserved aromatic residue in its B-type Greek key motif. We were able to identify several such proteins of the $\beta\gamma$-crystallin superfamily with identical substitutions in the genomes of several organisms. A few such sequences from bacteria and vertebrates are shown in Figure 9 with the consensus sequence GxWxxCxxxxY/FxGxC in the second Greek key motif. It appears that substitution of aromatic residue by Cys, as seen in caulollins and in other members, is not a random natural mutation but was naturally selected during evolution. This substitution of Cys does not affect binding of Ca^{2+} to caulollins. There is another Cys in many such variant Greek key motifs at the +2 position after Gly13 (Figure 9). A 3D model of caulollin-2D indicates that these two Cys residues, lying adjacent on two antiparallel β-strands, should be able to form an interstrand disulfide bond, which

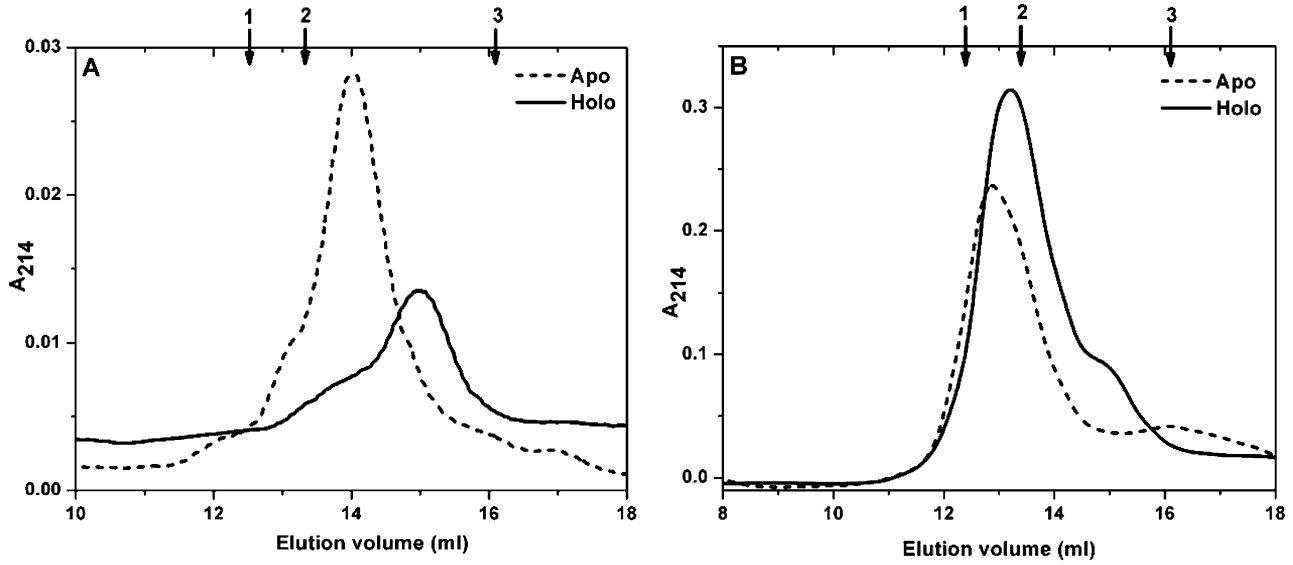

FIGURE 8: Analytical gel-filtration chromatography of (A) caulollin-2D and (B) caulollin-1. Elution volume of protein on Superdex 75 column was calibrated with molecular mass standards indicated by arrows: (1) chymotrpsinogen (25 kDa), (2) RNase A (13.7 kDa), and (3) insulin (5.8 kDa). For holoprotein elution, 5 mM $CaCl_2$ was added to the buffer to re-equilibrate the column.

Table 3: Thermodynamic Parameters of Thermal Protein Unfolding[a]

	T_m (°C)	ΔH_{cal} (kcal/mol)	ΔH_v (kcal/mol)	$\Delta Hv/\Delta H_{cal}$
caulollin-1 apo	55.3 ± 0.12	(2.98 ± 0.02) × 10^4	(3.0 ± 0.38) × 10^4	1.0
caulollin-1 holo	72.2 ± 0.08	(3.63 ± 0.04) × 10^4	(10.88 ± 0.17) × 10^4	2.9
caulollin-2D apo	57.2 ± 0.23	(1.23 ± 0.02) × 10^4	(2.97 ± 0.06) × 10^4	2.4
caulollin-2D holo	72.3 ± 0.02	(3.40 ± 0.01) × 10^4	(9.17 ± 0.06) × 10^4	2.7

[a] Derived from best fit to a two-state unfolding model.

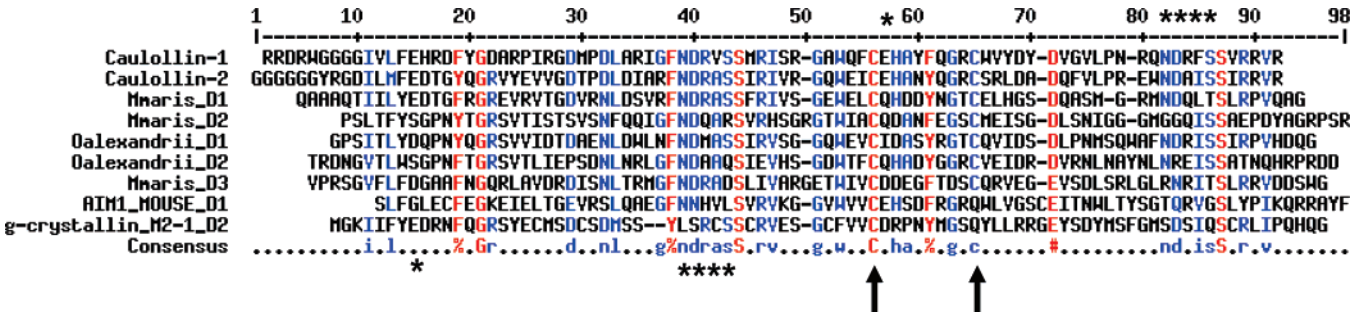

FIGURE 9: Sequence alignment of selected $\beta\gamma$-crystallins: The alignment shows the $\beta\gamma$-crystallin domain of caulollins along with other proteins of the superfamily in which aromatic residue is substituted by Cys (indicated by arrow). The proteins other than caulollins used for alignment are three $\beta\gamma$-crystallin domains (Mmaris_D1, Mmaris_D2, and Mmaris_D3) from the bacterium *Maricaulis maris* and two domains (Oalexandrii_D1 and Oalexandrii_D2) from the bacterium *Oceanicaulis alexandrii*. One domain (AIM1_MOUSE) from *Mus musculus* and one domain of γ-crystallin M2-1 ffrom metazoan *Petenia splendida* × *Cichlasoma synspilum* were also used. The sequences were aligned by use of MultAlin (*41*). Putative Ca^{2+}-binding residues identified by comparison with the sequence of protein S are indicated by asterisks.

is also predicted by the DISULFIND program (*39*). These proteins might have evolved an alternative to anchor the loop between a and b strands in a conformation competent for Ca^{2+} ligation, which could be a mechanism for redox-regulated function in these organisms. Our studies suggest that, in the absence of Ca^{2+}, this group of variant domains would adopt a partially unstructured conformation and that, upon binding Ca^{2+}, they would adopt the $\beta\gamma$-crystallin fold. Our results suggest that caulollins, along with other similar proteins, constitute a subclass within the Ca^{2+}-binding $\beta\gamma$-crystallin superfamily.

It is important to examine the relationship between sequence, stability, and evolutionary conservations within the $\beta\gamma$-crystallin fold as it has evolved to perform specialized biological functions. The $\beta\gamma$-crystallin domains of γ-crystallin, AIM-1, protein S, and spherulin 3a are structured and do not require Ca^{2+} to have a well-folded structure, though they all bind Ca^{2+} (*4*, *5*, *35*, *38*, *40*). On the other hand, a domain of *Yersinia* crystallin (domain D1) is intrinsically unstructured in the apo form and requires Ca^{2+} to have a proper $\beta\gamma$-crystallin fold (*6*). This is the only known domain in this superfamily that is completely unstructured in the apo form. In this work, we described $\beta\gamma$-crystallin domains that are partially unstructured and require Ca^{2+} for a structured fold. One interesting difference between structured and unstructured $\beta\gamma$-crystallin domains is the absence of the Tyr corner in the B-type Greek key motif. The Tyr corner has been proposed as a folding nucleus (*23*). However, some studies have indicated that the Tyr corner is essential for structural stability and not as a folding nucleus in β-barrel

proteins (*24*). Our studies support that the Tyr corner is essential for structural stability but can also be substituted by Ca^{2+}. Absence of the Tyr corner in $\beta\gamma$-crystallins might lead to structure in some cases or lack of structure in other proteins (*6*, *40*). However, conformation of unstructured $\beta\gamma$-crystallin domains is restored by Ca^{2+}, as seen in caulollins and *Yersinia* crystallin (*6*).

On the basis of various studies on $\beta\gamma$-crystallin domains, it appears that diverse $\beta\gamma$-crystallin domains could have distinct structural features and stabilities, and some of them require Ca^{2+} for the characteristic $\beta\gamma$-crystallin fold whereas others do not.

CONCLUSIONS

This work has added two more proteins to the list of growing numbers of Ca^{2+}-binding $\beta\gamma$-crystallin proteins with unique properties hitherto unpredicted from their sequence. Our data on this unique pair of $\beta\gamma$-crystallins from *C. crescentus* indicate that substitution of conserved residues is tolerable and does not affect Ca^{2+} binding. In fact, structure in these disordered proteins is restored by Ca^{2+}. Ca^{2+} ions usually stabilize loop regions, and we speculate a similar mechanism could be responsible for the increased stability of holocaulollins. Though Ca^{2+} plays important roles in the formation of the paracrystalline S-layer and in the physiology and reproduction of *C. crescentus*, no modulators or effectors have been described to date. One of the aims of genome sequencing of this bacterium was to identify such proteins (*16*). Availability of the genome sequence enabled us to identify and study a pair of Ca^{2+}-binding proteins in this bacterium that might act as a Ca^{2+} sensor in *Caulobacter* species. This work should enable others working on this bacterium to characterize the exact in vivo role of these Ca^{2+}-binding proteins in this widely studied prokaryotic model organism of cell division.

ACKNOWLEDGMENT

We gratefully thank Professor Lucy Shapiro and Dr. Ann Reisenauer, Stanford University, for the kind gift of *Caulobacter crescentus* CB15 genomic DNA, without which this work would not have been possible.

REFERENCES

1. Lubsen, N. H., Aarts, H. J., and Schoenmakers, J. G. (1988) The evolution of lenticular proteins: the β- and γ-crystallin super gene family, *Prog. Biophys. Mol. Biol. 51*, 47−76.
2. Wistow, G. (1990) Evolution of a protein superfamily: relationships between vertebrate lens crystallins and microorganism dormancy proteins, *J. Mol. Evol. 30*, 140−145.
3. Jaenicke, R., and Slingsby, C. (2001) Lens crystallins and their microbial homologs: structure, stability, and function, *Crit. Rev. Biochem. Mol. Biol. 36*, 435−499.
4. Rajini, B., Shridas, P., Sundari, C. S., Muralidhar, D., Chandani, S., Thomas, F., and Sharma, Y. (2001) Calcium binding properties of γ-crystallin: calcium ion binds at the Greek key beta gamma-crystallin fold, *J. Biol. Chem. 276*, 38464−38471.
5. Rajini, B., Graham, C., Wistow, G., and Sharma, Y. (2003) Stability, homodimerization, and calcium-binding properties of a single, variant $\beta\gamma$-crystallin domain of the protein absent in melanoma 1 (AIM1), *Biochemistry 42*, 4552−4559.
6. Jobby, M. K., and Sharma, Y. (2005) Calcium-binding crystallins from *Yersinia pestis*. Characterization of two single $\beta\gamma$-crystallin domains of a putative exported protein, *J. Biol. Chem. 280*, 1209−1216.
7. Barnwal, R. P., Jobby, M. K., Sharma, Y., and Chary, K. V. (2006) NMR assignment of M-crystallin: a novel Ca^{2+}-binding protein of the $\beta\gamma$-crystallin superfamily from *Methanosarcina acetivorans*, *J. Biomol. NMR 36* (Suppl 1), 32.
8. Clout, N. J., Kretschmar, M., Jaenicke, R., and Slingsby, C. (2001) Crystal structure of the calcium-loaded spherulin 3a dimer sheds light on the evolution of the eye lens $\beta\gamma$-crystallin domain fold, *Structure (Cambridge, MA, USA) 9*, 115−124.
9. Shimeld, S. M., Purkiss, A. G., Dirks, R. P., Bateman, O. A., Slingsby, C., and Lubsen, N. H. (2005) Urochordate $\beta\gamma$-crystallin and the evolutionary origin of the vertebrate eye lens, *Curr. Biol. 15*, 1684−1689.
10. Blundell, T., Lindley, P., Miller, L., Moss, D., Slingsby, C., Tickle, I., Turnell, B., and Wistow, G. (1981) The molecular structure and stability of the eye lens: x-ray analysis of gamma-crystallin II, *Nature 289*, 771−777.
11. Ray, M. E., Wistow, G., Su, Y. A., Meltzer, P. S., and Trent, J. M. (1997) AIM1, a novel non-lens member of the $\beta\gamma$-crystallin superfamily, is associated with the control of tumorigenicity in human malignant melanoma, *Proc. Natl. Acad. Sci. U.S.A. 94*, 3229−3234.
12. Marczynski, G. T., and Shapiro, L. (1995) The control of asymmetric gene expression during *Caulobacter* cell differentiation, *Arch. Microbiol. 163*, 313−321.
13. Jenal, U., and Stephens, C. (2002) The *Caulobacter* cell cycle: timing, spatial organization and checkpoints, *Curr. Opin. Microbiol. 5*, 558−563.
14. Nomellini, J. F., Kupcu, S., Sleytr, U. B., and Smit, J. (1997) Factors controlling in vitro recrystallization of the *Caulobacter crescentus* paracrystalline S-layer, *J. Bacteriol. 179*, 6349−6354.
15. Poindexter, J. S. (1984) The role of calcium in stalk development and in phosphate acquisition in *Caulobacter crescentus*, *Arch. Microbiol. 138*, 140−152.
16. Nierman, W. C., Feldblyum, T. V., Laub, M. T., Paulsen, I. T., Nelson, K. E., Eisen, J. A., Heidelberg, J. F., Alley, M. R., Ohta, N., Maddock, J. R., Potocka, I., Nelson, W. C., Newton, A., Stephens, C., Phadke, N. D., Ely, B., DeBoy, R. T., Dodson, R. J., Durkin, A. S., Gwinn, M. L., Haft, D. H., Kolonay, J. F., Smit, J., Craven, M. B., Khouri, H., Shetty, J., Berry, K., Utterback, T., Tran, K., Wolf, A., Vamathevan, J., Ermolaeva, M., White, O., Salzberg, S. L., Venter, J. C., Shapiro, L., Fraser, C. M., and Eisen, J. (2001) Complete genome sequence of *Caulobacter crescentus*, *Proc. Natl. Acad. Sci. U.S.A. 98*, 4136−4141.
17. Altschul, S. F., Gish, W., Miller, W., Myers, E. W., and Lipman, D. J. (1990) Basic local alignment search tool, *J. Mol. Biol. 215*, 403−410.
18. Jobby, M. K., and Sharma, Y. (2006) Purification of a crystallin domain of *Yersinia* crystallin from inclusion bodies and its comparison to native protein from the soluble fraction, *Biomed. Chromatogr. 20*, 956−963.
19. Maruyama, K., Mikawa, T., and Ebashi, S. (1984) Detection of calcium binding proteins by ^{45}Ca autoradiography on nitrocellulose membrane after sodium dodecyl sulfate gel electrophoresis, *J. Biochem. (Tokyo) 95*, 511−519.
20. Bohm, G., Muhr, R., and Jaenicke, R. (1992) Quantitative analysis of protein far UV circular dichroism spectra by neural networks, *Protein Eng. 5*, 191−195.
21. Wistow, G., Turnell, B., Summers, L., Slingsby, C., Moss, D., Miller, L., Lindley, P., and Blundell, T. (1983) X-ray analysis of the eye lens protein gamma-II crystallin at 1.9 A resolution, *J. Mol. Biol. 170*, 175−202.
22. Wistow, G., Jaworski, C., and Rao, P. V. (1995) A non-lens member of the beta gamma-crystallin superfamily in a vertebrate, the amphibian *Cynops*, *Exp. Eye Res. 61*, 637−639.
23. Hemmingsen, J. M., Gernert, K. M., Richardson, J. S., and Richardson, D. C. (1994) The tyrosine corner: a feature of most Greek key β-barrel proteins, *Protein Sci. 3*, 1927−1937.
24. Hamill, S. J., Cota, E., Chothia, C., and Clarke, J. (2000) Conservation of folding and stability within a protein family: the tyrosine corner as an evolutionary *cul-de-sac*, *J. Mol. Biol. 295*, 641−649.
25. Jobby, M. K., and Sharma, Y. (2007) Calcium-binding to lens βB2- and βA3-crystallins suggests that all β-crystallins are calcium-binding proteins, *FEBS J. 274*, 4135−4147.
26. Sharma, Y., Rao, C. M., Narasu, M. L., Rao, S. C., Somasundaram, T., Gopalakrishna, A., and Balasubramanian, D. (1989) Calcium ion binding to δ- and to β-crystallins. The presence of the "EF-hand" motif in δ-crystallin that aids in calcium ion binding, *J. Biol. Chem. 264*, 12794−12799.

27. Sharma, Y., and Balasubramanian, D. (1996) Calcium-binding properties of beta-crystallins, *Ophthalmic Res. 28* (Suppl. 1), 44−47.
28. Veenstra, T. D., Gross, M. D., Hunziker, W., and Kumar, R. (1995) Identification of metal-binding sites in rat brain calcium-binding protein, *J. Biol. Chem. 270*, 30353−30358.
29. Horrocks, W. D. Jr. (1993) Luminescence spectroscopy, *Methods Enzymol. 226*, 495−538.
30. Teintze, M., Inouye, M., and Inouye, S. (1988) Characterization of calcium-binding sites in development-specific protein S of *Myxococcus xanthus* using site-specific mutagenesis, *J. Biol. Chem. 263*, 1199−1203.
31. Trinkl, S., Glockshuber, R., and Jaenicke, R. (1994) Dimerization of beta B2-crystallin: the role of the linker peptide and the N- and C-terminal extensions, *Protein Sci. 3*, 1392−1400.
32. Ajaz, M. S., Ma, Z., Smith, D. L., and Smith, J. B. (1997) Size of human lens β-crystallin aggregates are distinguished by N-terminal truncation of betaB1, *J. Biol. Chem. 272*, 11250−11255.
33. Uversky, V. N. (2002) What does it mean to be natively unfolded? *Eur. J. Biochem. 269*, 2−12.
34. Hejtmancik, J. F., Wingfield, P. T., Chambers, C., Russell, P., Chen, H. C., Sergeev, Y. V., and Hope, J. N. (1997) Association properties of βB2- and βA3-crystallin: ability to form dimers, *Protein Eng. 10*, 1347−1352.
35. Rajini, B., and Sharma, Y. (2006) Domain-domain interaction and calcium-binding properties of a typical single $\beta\gamma$-crystallin domain of the protein Absent in Melanoma 1 (AIM1), *Calcium Binding Proteins 1*, 96−101.
36. Sturtevant, J. M. (1987) Biochemical applications of differential scanning calorimetry, *Annu. Rev. Phys. Chem. 38*, 463−488.
37. Stathopulos, P. B., Rumfeldt, J. A., Karbassi, F., Siddall, C. A., Lepock, J. R., and Meiering, E. M. (2006) Calorimetric analysis of thermodynamic stability and aggregation for apo and holo amyotrophic lateral sclerosis-associated Gly-93 mutants of superoxide dismutase, *J. Biol. Chem. 281*, 6184−6193.
38. Wenk, M., Baumgartner, R., Holak, T. A., Huber, R., Jaenicke, R., and Mayr, E. M. (1999) The domains of protein S from *Myxococcus xanthus*: structure, stability and interactions, *J. Mol. Biol. 286*, 1533−1545.
39. Ceroni, A., Passerini, A., Vullo, A., and Frasconi, P. (2006) DISULFIND: a disulfide bonding state and cysteine connectivity prediction server, *Nucleic Acids Res. 34*, W177−W181.
40. Rosinke, B., Renner, C., Mayr, E. M., Jaenicke, R., and Holak, T. A. (1997) Ca^{2+}-loaded spherulin 3a from *Physarum polycephalum* adopts the prototype gamma-crystallin fold in aqueous solution, *J. Mol. Biol. 271*, 645−655.
41. Corpet, F. (1988) Multiple sequence alignment with hierarchical clustering, *Nucleic Acids Res. 16*, 10881−10890.

BI700843Q